JHEP

Published for SISSA by Springer

Received: May 16, 2012
Revised: July 18, 2012
Accepted: July 26, 2012
Published: August 13, 2012

Finite volume treatment of $\pi\pi$ scattering and limits to phase shifts extraction from lattice QCD

M. Albaladejo,[a] **J.A. Oller,**[a] **E. Oset,**[b] **G. Rios**[a] **and L. Roca**[a]

[a] *Departamento de Física. Universidad de Murcia, E-30100 Murcia, Spain*

[b] *Departamento de Física Teórica and IFIC, Centro Mixto Universidad de Valencia-CSIC, Institutos de Investigación de Paterna, Aptdo. 22085, 46071 Valencia, Spain*

E-mail: albaladejo@um.es, oller@um.es, oset@ific.uv.es, g.rios.marquez@gmail.com, luisroca@um.es

Abstract: We study theoretically the effects of finite volume for $\pi\pi$ scattering in order to extract physical observables for infinite volume from lattice QCD. We compare three different approaches for $\pi\pi$ scattering (lowest order Bethe-Salpeter approach, N/D and inverse amplitude methods) with the aim of studying the effects of the finite size of the box in the potential of the different theories, specially the left-hand cut contribution through loops in the crossed $t, u-$channels. We quantify the error made by neglecting these effects in usual extractions of physical observables from lattice QCD spectrum. We conclude that for $\pi\pi$ phase-shifts in the scalar-isoscalar channel up to 800 MeV this effect is negligible for box sizes bigger than $2.5m_\pi^{-1}$ and of the order of 5% at around $1.5-2m_\pi^{-1}$. For isospin 2 the finite size effects can reach up to 10% for that energy. We also quantify the error made when using the standard Lüscher method to extract physical observables from lattice QCD, which is widely used in the literature but is an approximation of the one used in the present work.

Keywords: Lattice QCD, Chiral Lagrangians, Phenomenological Models

doi:10.1007/JHEP08(2012)071

JHEP08(2012)071

Contents

1 Introduction

One of the aims in present lattice QCD calculations is the determination of the hadron spectrum and many efforts are devoted to this task [1–25]. A recent review on the different methods used and results can be seen in [26]. Since one evaluates the spectrum for particles in a finite box, one must use a link from this spectrum to the physical one in infinite space. Sometimes, when it rarely happens, an energy level in a finite box rather independent of the volume is taken as a proof that this is the energy of a state in the infinite volume space. In other works the "avoided level crossing", with lines of spectrum that get close to each other and then separate, is usually taken as a signal of a resonance, but this criterion has been shown insufficient for resonances with a large width [27–29]. A more accurate method consists in the use of Lüscher's approach, but this works for resonances with only one decay channel. The method allows to reproduce the phase-shifts for the particles of this decay channel starting from the discrete energy levels in the box [30, 31]. This method has been recently simplified and improved in [29] by keeping the fully relativistic two-body propagator (Lüscher's approach makes approximations on the real part, *cf.* eqs. (3.1) and (3.2) below). The work of [29] also extends the method to two or more coupled channels. The extension to coupled channels has also been worked out in [32–34]. The work of [29] presents an independent method, which is rather practical, and has been tested and proved to work in realistic cases of likely lattice results. The method has been extended in [35] to obtain finite volume results from the Jülich model for the meson-baryon interaction and in [36] to study the interaction of the DK and ηD_s system where the $D_{s0}^*(2317)$ resonance is dynamically generated from the interaction of these particles. The case of the κ resonance in the $K\pi$ channel is also addressed in [37] following the approach of ref. [29]. It has also been extended to the case of interaction of unstable particles in [38], to the study of the DN interaction [39], the $\pi\pi$ interaction in the ρ channel [40] and to find strategies to determine the two $\Lambda(1405)$ states from lattice results [41].

JHEP08(2012)071

In ref. [29] the problem of getting phase-shifts and resonances from lattice QCD results ("inverse problem") using two coupled channels was addressed. Special attention was given to the evaluation of errors and the precision needed on the lattice QCD calculations to obtain phase-shifts and resonance properties with a desired accuracy. The derivation of the basic formula of [29] is done using the method of the chiral unitary approach [42] to obtain the scattering matrix from a potential. This method uses a dispersion relation for the inverse of the amplitude, taking the imaginary part of T^{-1} in the physical region and using unitarity in coupled channels [43, 44]. The method does not integrate explicitly over the left-hand cut singularity. Nevertheless, the latter might lead to interesting problems in finite volume calculations because in field theory, loops in the $t-$ or $u-$channel that contribute to crossed cuts, are volume dependent. There is no problem to incorporate these extra terms into the chiral unitary approach by putting them properly in the interaction kernel of the Bethe Salpeter equation or N/D method [43, 45], or using the inverse amplitude method (IAM) [46–51]. However, the method of [29] to analyze lattice spectrum and obtain phase-shifts explicitly relies upon having a kernel in the Bethe Salpeter equation which is volume independent. The same handicap occurs in the use of the standard Lüscher approach, where contributions from possible volume dependence in the potential are shown to be "exponentially suppressed" in the box volume. Yet, there is no way, unless one knows precisely the source of the volume dependent terms, to estimate these effects and determine for which volumes the "exponentially suppressed" corrections have become smaller than a desired quantity. This is however an important information in realistic calculations. The purpose of the present paper is to address this problem in a practical case, the scattering of pions in s-wave. For that we determine the strength of these volume dependent terms as a function of the size of the box and the impact of these effects in the determination of the phase-shifts in the infinite volume case.

The problem of $\pi\pi$ interaction in the lattice using the Lüscher approach has been studied for the case of $I = 2$, where one has no coupled channels and is technically easier for lattice calculations [52–54]. Along these lines in [55] a pioneer work is done of the problem that we address here performing a perturbative calculation at threshold for the cases of $I = 2$. Our approach is technically different, non perturbative, can be used for scattering energies and to evaluate phase shifts and is done for $I = 0$ and $I = 2$.

The contents of the paper are as follows. After this introduction, we summarize in section 2 the three models used to evaluate $\pi\pi$ scattering in the infinite and finite volume case. We then follow by studying the dependence on the lattice size of the box L of the resulting phase shifts in section 3. Conclusions are collected in section 4.

2 The $\pi\pi$ scattering in the finite box

In this section we explain the three models that we are going to consider in the present work to evaluate the $\pi\pi$ scattering within the chiral unitary approach: lowest order Bethe-Salpeter (BS), N/D and IAM. The latter two provide contributions to the left-hand cut of the scattering amplitude while the BS does not. After summarizing the models for the infinite volume, we explain for each of them how to evaluate the scattering in a box of finite

JHEP08(2012)071

size L. We study the scalar channel up to total energies of about 800 MeV for both isospin (I) 0 and 2. The isoscalar case is relevant for the lattice QCD studies of σ (or $f_0(500)$ [56]) meson resonance, while for the isotensor case the left-hand cut is more relevant (see below). Up to those energies the $K\bar{K}$ and $\eta\eta$ channels in the $I = 0$ case are negligible, hence, we deal here only with the $\pi\pi$ channel. The 4π channel, although open at lower energies around 555 MeV, is also neglected. Its effects were included in ref. [57] and the resulting inelasticity was negligible up to energies above 900 MeV. This extra intermediate state gives rise to L dependence that is not exponentially suppressed but, since phenomenologically is negligible in the energy range considered here, we do not expect any significant effects from this side. This channel was also neglected in the previous study of $\pi\pi$ scattering at threshold in finite volume [55] and its calculation is beyond our present aim. The 4π channel gives rise to a three-loop or $\mathcal{O}(p^8)$ contribution to the interaction kernel in Chiral Perturbation Theory (ChPT), while here we restrict ourselves to the one-loop or $\mathcal{O}(p^4)$ calculation of the interaction kernel. Indeed, any other volume dependence effect not considered by us in our present research is at least part of a two-loop calculation of the interaction kernel in ChPT.

2.1 Lowest order Bethe-Salpeter approach

In the chiral unitary approach the scattering matrix can be given by the Bethe-Salpeter equation in its factorized form [61]

$$T = [1 - VG]^{-1}V = [V^{-1} - G]^{-1}\,, \tag{2.1}$$

where V is the $\pi\pi$ potential, $V = -\frac{1}{f_\pi^2}(s - \frac{m^2}{2})$ for $I = 0$ and $V = \frac{1}{2f_\pi^2}(s - 2m^2)$ for $I = 2$, which are obtained from the lowest order chiral Lagrangians [62], with m the pion mass and $f_\pi = 92.4$ MeV. In eq. (2.1) G is the loop function of two meson propagators, which is defined as

$$G = i\int \frac{d^4p}{(2\pi)^4}\,\frac{1}{(P-p)^2 - m^2 + i\epsilon}\,\frac{1}{p^2 - m^2 + i\epsilon}\,, \tag{2.2}$$

with P the four-momentum of the global meson-meson system. Note that eq. (2.1) only has right-hand cut, unlike the other two approaches discussed in the next subsections.

The loop function in eq. (2.2) can be regularized either with dimensional regularization or with a three-momentum cutoff. The connection between both methods was shown in refs. [44, 51]. In dimensional regularization[1] the integral of eq. (2.2), G^D, is evaluated and gives for the $\pi\pi$ system [44, 63]

$$G^{\rm D}(E) = \frac{1}{(4\pi)^2}\left\{a(\mu) + \log\frac{m^2}{\mu^2} + \sigma\log\frac{\sigma+1}{\sigma-1}\right\}, \tag{2.3}$$

where $\sigma = \sqrt{1 - \frac{4m^2}{s}}$, $s = E^2$, with E the energy of the system in the center of mass frame, μ is a renormalization scale and $a(\mu)$ is a subtraction constant (note that only

[1] In our context we refer to the G function given in eq. (2.3) as calculated in "dimensional regularization". Of course, with the latter procedure the result is infinite. The infinite is removed by the subtraction constant $a(\mu)$. A more accurate formulation can be given in terms of dispersion relations, the interested reader on this point can consult refs. [43, 44], though the final result is the same.

JHEP08(2012)071

the combination $a(\mu) - \log \mu^2$ is the relevant degree of freedom, that is, there is only one independent parameter).

The loop function G can also be regularized with a three momentum cutoff $p_{\rm max}$ and, after the p^0 integration is performed [61], it results

$$G(s) = \int\limits_{|\vec{p}|<p_{\rm max}} \frac{d^3\vec{p}}{(2\pi)^3} \frac{1}{\omega(\vec{p})} \frac{1}{s - 4\omega(\vec{p})^2 + i\epsilon} ,$$

$$\omega(\vec{p}) = \sqrt{m^2 + \vec{p}^{\,2}} . \tag{2.4}$$

Let us now address the modifications in order to evaluate the $\pi\pi$ scattering in a finite box following the procedure explained in ref. [29]. The main difference with respect to the infinite volume case is that instead of integrating over the energy states of the continuum with $\vec{p}$ being a continuous variable as in eq. (2.4), one must sum over the discrete momenta allowed in a finite box of side L with periodic boundary conditions. We then have to replace G by $\widetilde{G}$, where

$$\widetilde{G} = \frac{1}{L^3} \sum_{\vec{p}}^{|\vec{p}|<p_{\rm max}} \frac{1}{\omega(\vec{p})} \frac{1}{s - 4\omega(\vec{p})^2} ,$$

$$\vec{p} = \frac{2\pi}{L} \vec{n} , \quad \vec{n} \in \mathbb{Z}^3 \tag{2.5}$$

For the sake of comparison with the other models considered in the present work, where dimensional regularization is always done, we use the procedure of [36] in order to write the finite volume loop function $\widetilde{G}$ in terms of the infinite volume one G^D evaluated in dimensional regularization:

$$\widetilde{G}^D = G^{\rm D} + \lim_{p_{\rm max}\to\infty} \left[\frac{1}{L^3} \sum_{\vec{p}_i}^{p_{\rm max}} I(\vec{p}_i, s) - \int\limits_{p<p_{\rm max}} \frac{d^3\vec{p}}{(2\pi)^3} I(\vec{p}, s) \right] , \tag{2.6}$$

where $I(\vec{p}, s)$ is the integrand of eq. (2.4),

$$I(\vec{p}, s) = \frac{1}{\omega(\vec{p})} \frac{1}{s - 4\omega(\vec{p})^2} . \tag{2.7}$$

Note that $\widetilde{G}^D$ of eq. (2.6) depends on the subtraction constant a instead of the three-momentum cutoff $p_{\rm max}$. The dependence on the latter cancels in the difference between the two terms in the square brackets of eq. (2.6).

In the box the scattering matrix reads

$$\widetilde{T} = \frac{1}{V^{-1} - \widetilde{G}^D} . \tag{2.8}$$

The eigenenergies of the box correspond to energies that produce poles in the $\widetilde{T}$ matrix, which corresponds to the condition $\widetilde{G}^D(E) = V^{-1}(E)$. Therefore for those values of the energies, the T matrix for infinite volume can be obtained by

$$T(E) = \left(V^{-1}(E) - G^D(E)\right)^{-1} = \left(\widetilde{G}^D(E) - G^D(E)\right)^{-1} . \tag{2.9}$$

JHEP08(2012)071

The amplitude is related to the phase-shifts by

$$T(E) = -\frac{8\pi E}{p}\frac{1}{\cot\delta - i}\,, \tag{2.10}$$

where $p = \frac{E}{2}\sqrt{1-\frac{4m^2}{s}}$ is the CM momentum.

Eq. (2.9) is nothing but Lüscher formula [30, 31] except that, as shown in ref. [29], eq. (2.9) keeps all the terms of the relativistic two-body propagator, while Lüscher's approach neglects terms in Re $I(p)$ which are exponentially suppressed in the physical region, but can become sizable below threshold, or in other cases when small volumes are used or large energies are involved.

We would like to make the following observation here. Let us consider eq. (2.9) in the cutoff regularization procedure. We would obtain

$$T(E) = (\widetilde{G} - G)^{-1} \tag{2.11}$$

with G and $\widetilde{G}$ given by eqs. (2.4) and (2.5) respectively. In the application to Quantum Mechanics of Lüscher formalism, the cutoff would be playing the effect of a finite range. However, one should note that the difference $\widetilde{G} - G$ has a finite limit when the cutoff goes to infinity and this is what the Lüscher formalism assumes. Note that the difference of the part of the sum and integral from $p_{\rm max}$ to infinity goes rapidly to zero as $p_{\rm max}$ increases, leading to terms exponentially suppressed in L. So, to make the limit of $p_{\rm max}$ infinite in eq. (2.11) is within the usual assumptions in the derivation of Lüscher formula and makes the results cutoff independent. Then eq. (2.11) in the limit of $p_{\rm max} \to \infty$ is exactly Lüscher formula, up to the relativistic corrections that we have mentioned. On the other hand, in lattice QCD calculations the information on $p_{\rm max}$ does not exist since the cutoff is implicitly infinite and divergences of the theory are reabsorbed in some physical observable. In this sense a rederivation of the improved Lüscher formula, eq. (2.9), without invoking cutoffs is advisable and this is done in [36] (eqs. (11) to (17) of that paper), with the dimensional regularized G functions. This is what we have used in eq. (2.6) and throughout the paper.

2.2 The IAM approach

The next approach considered is the elastic IAM [46–50], which we briefly review in this section and describe how to extend it to consider scattering in a finite box.

The elastic IAM makes use of elastic unitarity and ChPT [62] to evaluate a dispersion relation for the inverse of the $\pi\pi$ scattering partial wave of definite isospin I and angular momentum J, T^{IJ} (in the following we drop the superscript IJ to simplify notation). The advantage of using the inverse of a partial wave stems from the fact that its imaginary part is fixed by unitarity,

$$\mathrm{Im}\, T = -\frac{\sigma}{16\pi}|T|^2 \quad \Rightarrow \quad \mathrm{Im}\, T^{-1} = \frac{\sigma}{16\pi}\,. \tag{2.12}$$

Thus, the right-hand cut integral can be evaluated exactly in the elastic regime and the obtained partial wave satisfies unitarity exactly. The partial wave amplitudes calculated in ChPT cannot satisfy unitarity exactly since they are obtained in a perturbative expansion

JHEP08(2012)071

$T = T_2 + T_4 + \mathcal{O}(p^6)$, where $T_2 = \mathcal{O}(p^2)$ and $T_4 = \mathcal{O}(p^4)$ are the Leading Order and Next-to-Leading Order contributions in the chiral expansion of T, respectively. However, unitarity is satisfied in a perturbative way,

$$\mathrm{Im}\, T_2 = 0, \quad \mathrm{Im}\, T_4 = -\frac{\sigma}{16\pi} T_2^2, \quad \cdots . \tag{2.13}$$

These equations allow us to evaluate the dispersion relation and obtain a compact form for the partial wave as we show below.

We write then a dispersion relation for an auxiliary function $F \equiv T_2^2/T$, whose analytic structure consists on a right-hand cut (RC) from $4m_\pi^2$ to ∞, a left-hand cut (LC) from $-\infty$ to 0, and possible poles coming from zeros of T,

$$F(s) = F(0) + F'(0)s + \frac{1}{2}F''(0)s^2 + \frac{s^3}{\pi}\int_{RC} ds' \frac{\mathrm{Im}\, F(s')}{s'^3(s'-s)} + LC(F) + PC\,, \tag{2.14}$$

where we have performed three subtractions to ensure convergence. In the above equation $LC(F)$ stands for the integral over the left-hand cut, and PC stands for possible poles contributions, which are present in the scalar waves due to the Adler zeros. Using eqs. (2.12) and (2.13) we can evaluate *exactly* in the RC integral $\mathrm{Im}\, F = -\mathrm{Im}\, T_4$, and obtain for the right-hand cut $RC(F) = -RC(T_4)$. The subtraction constants can be evaluated with ChPT since they only involve amplitudes or their derivatives evaluated at $s = 0$, $F(0) \simeq T_2(0) - T_4(0)$, $F'(0) \simeq T_2'(0) - T_4'(0)$, $F''(0) \simeq -T_4''(0)$. The left-hand cut can be considered to be dominated by its low energy part, since we have three subtractions, and it is also dumped by an extra $1/(s'-s)$ when considering physical values of s. Then, we evaluate it using ChPT to obtain $LC(F) \simeq -LC(T_4)$. The pole contribution is formally $\mathcal{O}(p^6)$ and we neglect it (this causes some technical problems in the subthreshold region around the Adler zeros which can be easily solved, but they do not affect the description of scattering or resonances, for details see [64]). Taking into account all the above considerations we arrive at

$$\frac{T_2^2(s)}{T(s)} \simeq T_2(0) + T_2'(0)s - T_4(0) - T_4'(0)s - \frac{1}{2}T_4''(0)s^2 \quad - RC(T_4) - LC(T_4) = T_2(s) - T_4(s)\,, \tag{2.15}$$

where in the last step we have taken into account that $T_2(s)$ is just a first order polynomial in s so that $T_2(s) = T_2(0) + T_2'(0)s$, and that the remaining piece in the middle member of eq. (2.15) is a dispersion relation for $-T_4(s)$. Then one obtains the simple IAM formula,

$$T^{IAM} = \frac{T_2^2}{T_2 - T_4}\,. \tag{2.16}$$

This formula can be systematically extended to higher orders by evaluating the subtraction constants and the left-hand cut in the dispersion relation to higher orders. Note that the full one-loop ChPT calculation is used, so the IAM partial waves depend on the chiral Low Energy Constants (LECs), that absorb the loop divergences through their renormalization and depend on a renormalization scale μ. Of course, this μ dependence is canceled out in physical observables. In the case of $\pi\pi$ scattering there appear four LECs, denoted $l_i^r(\mu)$,

JHEP08(2012)071

$i = 1 \ldots 4$. These LECs are not fixed from symmetry considerations and their value has to be determined from experiment. For the IAM calculations here we take the values used in [65]: $10^3 l_1^r = -3.7 \pm 0.2$, $10^3 l_2^r = 5.0 \pm 0.4$, $10^3 l_3^r = 0.8 \pm 3.8$, $10^3 l_4^r = 6.2 \pm 5.7$, at $\mu = 770\,\text{MeV}$, which give a good description of phase-shift data. Note that in the present work we are not interested in a detailed description of scattering data, but on the effects of ignoring the exponentially suppressed dependence on the box size when using Lüscher's or the chiral unitary approach to obtain the scattering phase-shifts from the energy levels in finite volume.

Both in the IAM and the N/D method (explained below) the dependence with the finite size of the box enters through the chiral amplitude $A_4(s,t,u)$, which is used to calculate the partial waves at $\mathcal{O}(p^4)$, denoted by T_4. This amplitude receives contributions from loop diagrams, whose momentum integrals should be replaced by discrete sums over the allowed momenta in the finite box. In particular, these contributions come from s-, t- and u-channel loop diagrams, figure 1(b), (c) and (d), respectively, and from tadpole diagrams, figure 1(a). Note also that we write the amplitudes in terms of the physical pion mass m_π and decay constant f_π, so that the NLO contributions to them are included as $\mathcal{O}(p^4)$ terms in the amplitude T_4. The $O(p^4)$ $\pi\pi$ scattering amplitude $A_4(s,t,u)$ can be generically written, both for $I = 0$ and $I = 2$, in terms of only two one-loop functions G and H:

$$A_4(s,t,u) = P_L + P_H H(m^2) + P_{G,s} G(s) + P_{G,t} G(t) + P_{G,u} G(u)\,, \tag{2.17}$$

where P_X are polynomials of the Mandelstam variables. In particular, the LECs appear only in P_L. In the above equation, H and $G(P^2)$ are the one- and two-point one loop functions, respectively:

$$G(P^2) = \int \frac{d^3\vec{q}}{(2\pi)^3} \frac{\omega_{\vec{q}} + \omega_{\vec{P}-\vec{q}}}{2\omega_{\vec{q}}\omega_{\vec{P}-\vec{q}}} \frac{1}{(P^0 - \omega_{\vec{q}} - \omega_{\vec{P}-\vec{q}})(P^0 + \omega_{\vec{q}} + \omega_{\vec{P}-\vec{q}})}, \tag{2.18}$$

$$H = \int \frac{d^3\vec{q}}{(2\pi)^3} \frac{1}{2\omega_{\vec{q}}}, \tag{2.19}$$

and P is the four-momentum entering the loop so that $G(s)$, $G(t)$ and $G(u)$ in eq. (2.17) arise from the s-, t- and u-channel loops (2.18) with $P^2 = s$, t and u respectively. In dimensional regularization and after the divergences and scale dependencies are absorbed in the LECs [62], the loop functions then read

$$G^R(P^2) = \frac{1}{16\pi^2}\left(-1 + \sigma(P^2)\log\frac{1+\sigma(P^2)}{1-\sigma(P^2)}\right), \tag{2.20}$$

with $\sigma(P^2) = \sqrt{1 - 4m_\pi^2/P^2}$. On the other hand, because of the regularization approach followed, we have $H^R = 0$ (see e.g. ref. [66]). The partial waves T_4 are then obtained by projecting the $I = 0$ or $I = 2$ amplitude A_4 on angular momentum J.

The s-channel loops are responsible for the right unitarity cut, and contain the most important L dependence of the amplitude. This L dependence coming from the unitarity cut is the one used by the Lüscher/chiral unitary approach method to obtain the phase-shift from the energy levels in a finite volume. However, the t- and u-channel loops (which give

JHEP08(2012)071

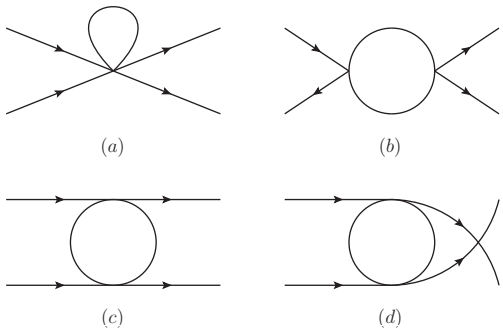

Figure 1. Loop contributions to the $O(p^4)$ chiral $\pi\pi$ scattering amplitude T_4. The s-channel loop (b) gives rise to the right unitarity cut, whereas the t- and u-channel loops, (c) and (d), contribute to the left-hand cut. Diagram (a) gives rise to the tadpole contributions.

rise to the left-hand cut when projecting into partial waves) and the tadpoles, give an extra dependence on L (polarization corrections in the terminology of ref. [31]) that is neglected in the Lüscher/chiral unitary approach method since it is exponentially suppressed.

Then, the IAM amplitudes in finite volume are calculated replacing $T_4(s)$ in eq. (2.16) with $\widetilde{T}_4(s)$, which is the s-wave projection of the $I = 0$ or $I = 2$ $\pi\pi$ scattering amplitude in finite volume $\widetilde{A}_4(s,t,u)$. The latter is obtained from eq. (2.17), but replacing the loop functions in eqs. (2.18) and (2.19) with their finite volume counterparts, $\widetilde{G}^R$ and $\widetilde{H}^R$. Following again the procedure in [36] (see also the discussion at the end of subsection 2.1), we obtain the finite volume loop functions from the infinite volume ones as

$$\widetilde{G}^R(P) = G^R(P^2) + \lim_{q_{\max}\to\infty}\left[\frac{1}{L^3}\sum_{\vec{q}_i}^{q_{\max}} I(\vec{q}_i,P) - \int_{q<q_{\max}} \frac{d^3\vec{q}}{(2\pi)^3} I(\vec{q},P)\right], \tag{2.21}$$

$$\widetilde{H}^R = H^R + \lim_{q_{\max}\to\infty}\left[\frac{1}{L^3}\sum_{q_i}^{q_{\max}} \frac{1}{2\omega_{\vec{q}}} - \int_{q<q_{\max}} \frac{d^3\vec{q}}{(2\pi)^3}\frac{1}{2\omega_{\vec{q}}}\right], \tag{2.22}$$

where $I(\vec{q},P)$ is the integrand of eq. (2.18),

$$I(\vec{q},P) = \frac{\omega_{\vec{q}}+\omega_{\vec{P}-\vec{q}}}{2\omega_{\vec{q}}\omega_{\vec{P}-\vec{q}}}\frac{1}{(P^0-\omega_{\vec{q}}-\omega_{\vec{P}-\vec{q}})(P^0+\omega_{\vec{q}}+\omega_{\vec{P}-\vec{q}})}. \tag{2.23}$$

Note that the box breaks Lorentz symmetry and fixes the reference frame to the center of mass frame of the initial pions. For this reason we have used P as the argument of $\widetilde{G}^R$ in eq. (2.21) instead of P^2.

In the case of the s-channel loop, where $\vec{P} = 0$ so that $(P^0)^2 = P^2 = s$, we obtain $\widetilde{G}^R(P)$ as in eqs. (2.6) and (2.7), but with G^D replaced by G^R. Note that $\widetilde{G}^R(P)$ in this case only depends on $P^2 = s$. For the t-channel loop, where $P^0 = 0$ so that $P^2 = -\vec{P}^2 = t$, the integrand $I(\vec{q},P)$ reduces to

$$I(\vec{q},P) = -\frac{1}{2\omega_{\vec{q}}\omega_{\vec{P}-\vec{q}}(\omega_{\vec{q}}+\omega_{\vec{P}-\vec{q}})}, \tag{2.24}$$

JHEP08(2012)071

but now, contrary to the s-channel case, $G(P)$ not only depends on $P^2 = t$, but also on $\vec{P}$ and its relative orientation respect to the cubic lattice of allowed momenta in the box, $\{\vec{q}_i\}$. In the end this translates into a dependence on the scattering angle θ, already present in $t = -2(s/4 - m_\pi^2)(1 - \cos\theta)$, but also on the azimuthal angle ϕ, and this also happens with the u-channel case. Thus, when projecting into s-wave, $T(s) = \frac{1}{2}\int d(\cos\theta) A(s, \cos\theta)$, we should now also integrate on ϕ, $T(s) = \frac{1}{4\pi}\int d\phi \int d(\cos\theta) A(s, \cos\theta, \phi)$, where θ and ϕ are the polar and azimutal angles of the final three-momentum entering in $\vec{P}$. The scalar product $\vec{P}\cdot\vec{q}$ in eq. (2.24) can be expressed in spherical coordinates in an standard way and then inserted in the equation above for the angular projection, including the ϕ integration. Finally, $\widetilde{H}^R$ can be evaluated using the Poisson resummation formula (see e.g. [55]) and taking into account that $H^R = 0$ we obtain

$$\widetilde{H}^R = \frac{m_\pi}{4\pi^2 L} \sum_{0\neq\vec{n}\in\mathbb{Z}^3} \frac{1}{|\vec{n}|} K_1(|\vec{n}| m_\pi L), \tag{2.25}$$

where K_1 is the Bessel function.

Now, the energy levels in the box are obtained from the poles in the scattering partial wave, eq. (2.16), or equivalently, the zeros of $T_2(s) - \widetilde{T}_4(s)$. From these energy levels at several values of L one can re-obtain the phase-shifts for the infinite volume with the Lüscher/chiral unitary approach method, and compare them with the exact infinite volume result to quantify the effect of neglecting the L dependence coming from the crossed channel loops and tadpoles.

2.3 The N/D method

The case presented in subsection 2.1 can be put in the more general framework of the N/D method [43, 44, 57–60, 67]. The amplitude was denoted by $T(s)$ in eq. (2.1). This master formula is obtained by solving algebraically the N/D method [43, 44, 67, 68], with the crossed cuts treated perturbatively, while the right-hand cut is resummed exactly. The different chiral orders of $V(s) = V_2(s) + V_4(s) + \ldots$ are calculated by matching $T(s)$ with the perturbative amplitudes $T_n(s)$. In this way, up to $\mathcal{O}(p^4)$,

$$\begin{aligned} T(s) &= \frac{V(s)}{1 - V(s)G^D(s)} \\ &= T_2(s) + T_4(s) + \ldots \\ &= V_2(s) + V_4(s) + V_2(s)^2 G^D(s) + \ldots , \end{aligned} \tag{2.26}$$

where the ellipsis indicates $\mathcal{O}(p^6)$ and higher orders in the expansion. It results then:

$$\begin{aligned} V_2(s) &= T_2(s)\,, \\ V_4(s) &= T_4(s) - T_2(s)^2 G^D(s)\ . \end{aligned} \tag{2.27}$$

The finite piece of the unitarity term in the $\pi\pi$ chiral amplitude is given by:

$$T_4^U(s) = T_2(s)^2 G^R(s)\,, \tag{2.28}$$

JHEP08(2012)071

with $G^R(s)$ given in eq. (2.20). In this way, the kernel $V(s) = V_2(s)+V_4(s)$ has no unitarity cut because:

$$T_4^U(s) - T_2(s)^2 G^D(s) = T_2(s)^2 (G^R(s) - G^D(s)) \,, \tag{2.29}$$

and the cut is cancelled in the r.h.s. of the previous equation. The full right-hand cut stems then from the denominator $1 - V(s)G^D(s)$ in eq. (2.1).

In the infinite volume case, the LECs are fixed to experiment, as well as the subtraction constant a. We use here the central values of the fit given in [66], for which the values of the finite and scale independent LECs $\bar{l}_i$ are $\bar{l}_1 = 0.8 \pm 0.9$, $\bar{l}_2 = 4.6 \pm 0.4$, $\bar{l}_3 = 2 \pm 4$, $\bar{l}_4 = 3.9 \pm 0.5$. In terms of the latter, the so-called renormalized LECs, which depend on the renormalization scale, are $10^3 l_1^r = -2.8 \pm 0.9$, $10^3 l_2^r = 2.5 \pm 0.8$, $10^3 l_3^r = 2 \pm 6$, $10^3 l_4^r = 3 \pm 3$, where the renormalization scale is chosen at $\mu = 770$ MeV. The subtraction constant a takes the value $a = -1.2 \pm 0.4$. We additionally note here that the same subtraction constant is used for both channels, as required by isospin symmetry [69].

In order to study the finite volume scattering, the same replacements as in the IAM and BS methods must be done. In particular, in the kernel $V(s) \to \widetilde{V}(s)$ no change is needed in $V_2(s)$, whereas $V_4(s)$ is changed to $\widetilde{V}_4(s)$,

$$\widetilde{V}_4(s) = \widetilde{T}_4(s) - T_2(s)^2 \widetilde{G}^D(s) \,. \tag{2.30}$$

Notice that, in view of eq. (2.29), there is no finite volume effect in the s-channel contributions to the kernel $\widetilde{V}(s)$. The volume dependence enters then in the kernel through the t- and u-channel loop functions and tadpoles evaluated as discussed in section 2.2. The s-channel volume dependence enters then at the denominator of the amplitude

$$\widetilde{T}(s) = \frac{\widetilde{V}(s)}{1 - \widetilde{V}(s)\widetilde{G}^D(s)} \tag{2.31}$$

through the function $\widetilde{G}^D(s)$ in its version of eq. (2.6), which gives the most important contribution to the aforementioned dependence, as in the case of the IAM method. The change in the values of the subtraction constant a with L is not considered because this is accounted for by employing $\widetilde{G}^D(s)$, eq. (2.6).

3 Results

As already explained, the main aim of the present work is to quantify the effect of the dependence of the different potentials considered on the size of the box, L. Hence, we are going to compare the L dependence of the N/D and the IAM methods with that of the BS, the kernel of which does not depend on L.

First we show in figure 2 the results for the $\pi\pi$ phase-shifts in s-wave and $I = 0$ for the three different models in infinite volume. The IAM and N/D results (solid and dashed lines, respectively) are the fits explained in the previous section and the BS (dot-dashed line) is fitted in this work to the experimental data [70–75] shown in the figure up to 800 MeV. The IAM and N/D approaches are essentially equivalent at low energies but differ slightly as the energy increases. Thus the difference between the IAM and N/D phase shifts is mainly

JHEP08(2012)071

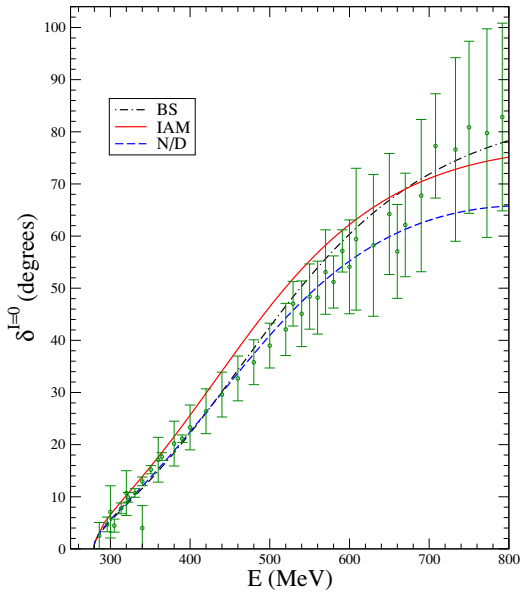

Figure 2. Isospin I=0, s-wave, $\pi\pi \to \pi\pi$ phase-shifts for the three different models considered: solid, dashed and dot-dashed lines correspond to IAM, N/D and BS, respectively. The experimental data are from refs. [70–75].

due to the different set of data used in the fit and it also gives an idea of the theoretical uncertainty. The BS approach produces a curve in between the other two, closer to the N/D at low energies and to the IAM at higher energies. In any case, the different models are compatible within the experimental uncertainties. Let us note that what matters for the discussions in the present work is not the actual values of the phase-shifts at infinite volume but the relative change when going to the finite box.

In figure 3 we show the energy levels for different values of the cubic box size, L, for the different models which have been obtained from the zeroes of the scattering amplitudes in the finite box as explained in the previous section. The dotted lines represent the free $\pi\pi$ energies in the box, while the other lines correspond to IAM, N/D and BS as in figure 2.

The differences are very small for the largest values of L shown in the plot but are more important for smaller L, specially between the N/D and IAM methods. The BS approach produces a curve in between the other two, closer to the N/D. The IAM and BS are more similar for larger values of energies as can also be seen in the phase shifts, figure 2. As an example of small L, we note that for $L = 1.7 m_\pi^{-1}$ the difference between N/D and IAM is about 30 MeV.

An actual lattice calculation would provide some points over analogous trajectories in the E vs. L plots. The "inverse problem" is the problem of getting the actual scattering amplitudes (and hence by-product magnitudes like phase-shifts) in the infinite space from data produced by lattice QCD consisting of points in plots of E vs. L over the energy levels in the box. For points in these levels the amplitude in the infinite volume can be extracted from the generalization of the Lüscher formula, as explained in the previous sections, see eq. (2.9).

JHEP08(2012)071

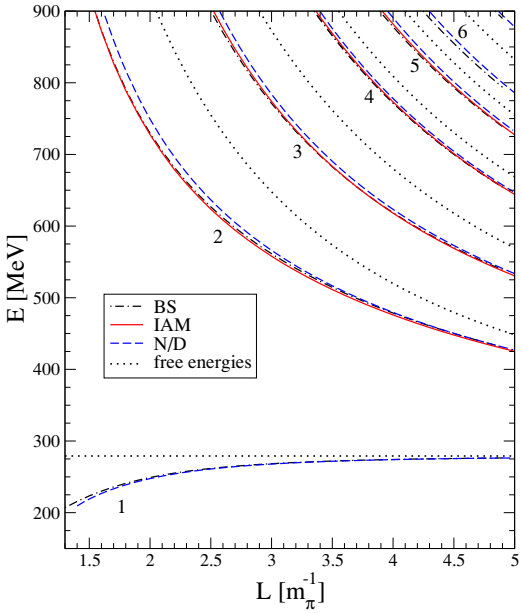

Figure 3. The first energy levels as a function of the cubic box size L for the three different models considered for $I = 0$. The dotted lines indicate the free $\pi\pi$ energies in the box. The rest of the lines correspond to IAM, N/D and BS as in figure 2.

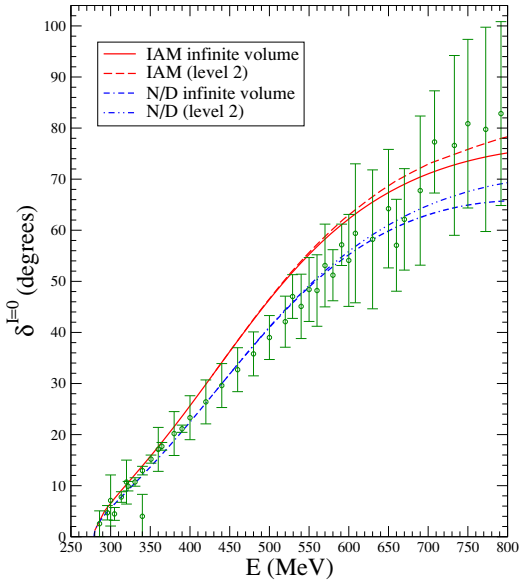

Figure 4. Solution of the inverse problem for $I = 0$ for the IAM and N/D methods. The BS result is the same as in the infinite volume case and thus we do not show it in the figure. We show the results obtained only from level 2 of figure 3 since the results with levels > 2 almost overlap with the infinite volume line. For the meaning of each line consult the inset in the figure.

In figure 4 we show the phase-shifts obtained for the different methods implementing the "inverse problem" analysis (or "reconstructed" results) with eq. (2.9) and from the E vs. L plot. For the BS model the results are independent of the level used for a given E, since the potential does not depend on L, and they are equal to the infinite volume result.

JHEP08(2012)071

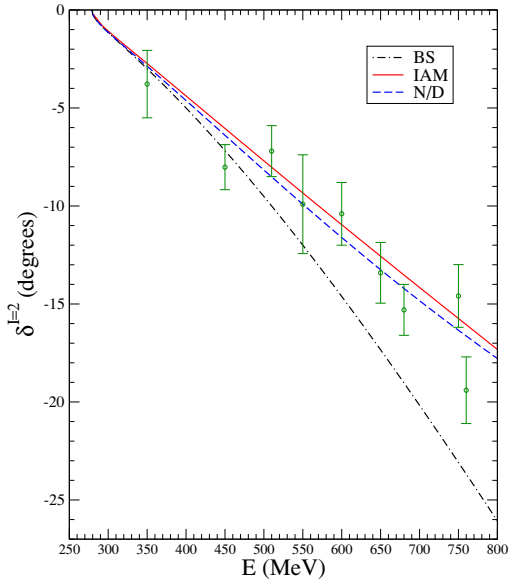

Figure 5. Isospin I=2, s-wave, $\pi\pi \to \pi\pi$ phase-shifts for the three different models considered. The experimental data are from refs. [76, 77]. See the inset in the figure for the correspondence between the different lines and the approach used.

Therefore we do not show the BS result since it is the same as in figure 2. For the IAM and N/D methods the results depend on the level chosen for a given E since the potentials depend on L as explained in the previous sections. Actually, for levels > 2 of figure 3 the results are almost equal to the infinite volume results and hence we do not show them in the figure since they would almost overlap with the infinite volume line. This is because, as seen in figure 3, for the higher energies these levels imply large values of L. Indeed, for energies below 800 MeV this implies values of L higher than about $3m_\pi^{-1}$. For the results obtained with level 2, the phase-shifts differ in about 5% of the result in the infinite volume at the higher energies considered. For $E \sim 800$ MeV this implies L values slightly smaller than $2m_\pi^{-1}$, as can be seen in figure 3. It is worth noting that the effect of the dependence on L of the models with left-hand cut go in the same direction and are of similar size in spite of the different models used. This gives us confidence that the actual L dependence of the left-hand cut is properly considered and the real effect of any realistic model would be of the order obtained in the present work. An analysis with eq. (2.9) applied to actual lattice results of E versus L levels would neglect the possible L dependence of the potential and hence the errors from the L dependence of the left-hand cut would be of the order of the differences shown in the figure. Note also that the L dependence of the results are smaller than the initial difference between the N/D and IAM themselves and also lower than the experimental uncertainties. Therefore, an actual lattice calculation should care about this L dependence only if it aims at getting errors smaller than the effect obtained in the present work.

In figures 5, 6 and 7 we show for the $I = 2$ case the same results as in figures 2 to 4 for $I = 0$. In figure 5 we see that the IAM and N/D methods provide very similar results and compatible with the experimental data while the BS approach gets worse phase-shifts.

JHEP08(2012)071

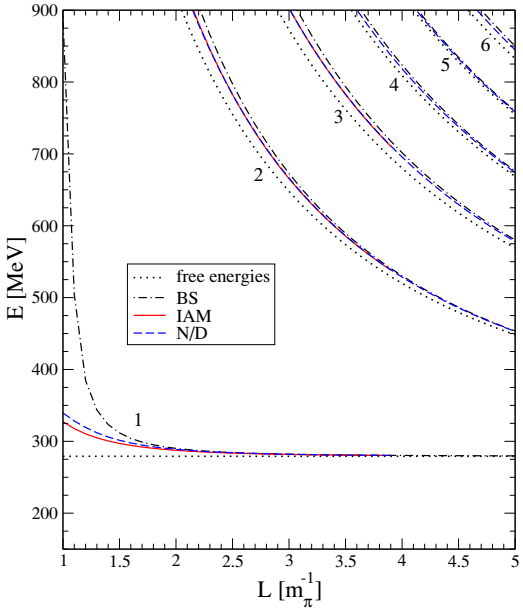

Figure 6. The first energy levels as a function of the cubic box size L for the three different models considered for $I = 2$. The meaning of the different lines is as in figure 3.

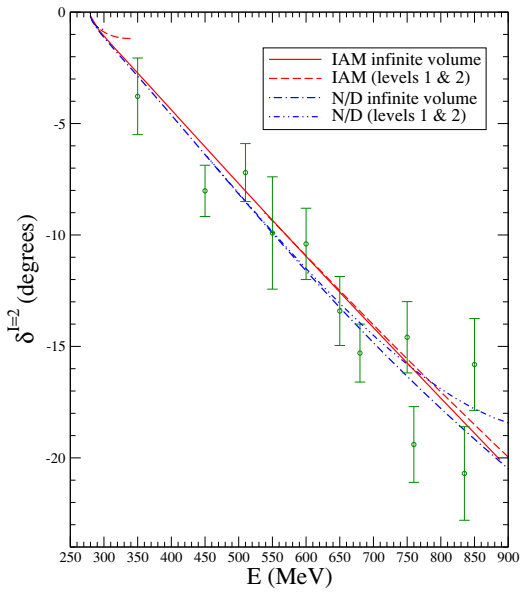

Figure 7. Solution of the inverse scattering problem with $I = 2$ for the IAM and N/D methods. The BS result is the same as in the infinite volume case and thus we do not show it in the figure. We show the results obtained only from level 1 and 2 of figure 6 since the results with levels > 2 almost overlap with the infinite volume line. For the meaning of the lines consult the inset in the figure.

This is because in the IAM and N/D the left-hand cut is included perturbatively order by order, unlike the BS model, and in this channel the left-hand cut is more relevant. In figure 6 we show the energy levels in the box for this channel.

Now both IAM and N/D provide similar results. In figure 7 we show the solution of the inverse problem for the phase-shifts. We see that the N/D method provides a higher

JHEP08(2012)071

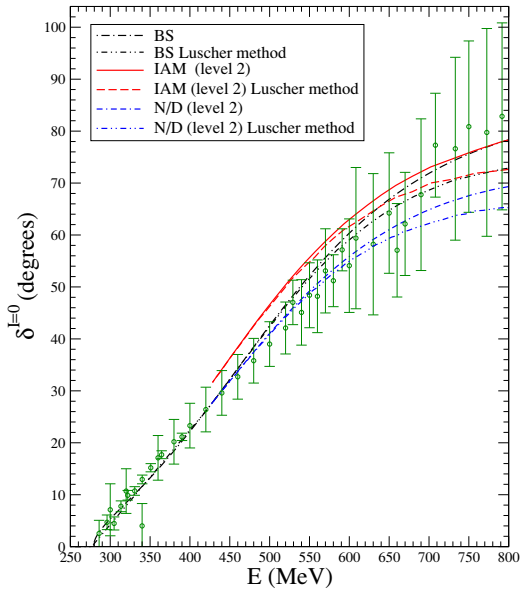

Figure 8. Difference between the inverse method formula, eq. (2.9), and the approximated Lüscher formula. The approach corresponding to each line is given in the inset in the figure.

L dependence for large values of the energies, unlike IAM. At 800 MeV the difference is about 10% for the N/D and 2% for the IAM. The difference in the phase-shifts between the two approaches is large in spite of the energy levels being very similar. This is because the energy levels are very close to the free case, unlike the $I = 0$ case, and then the $\widetilde{G}$ function is very steep. This makes that small variations in E provide large variations in $\widetilde{G}$.

In usual inverse problem analysis from actual lattice results, it is common to use the Lüscher formula [30, 31] which, as explained in section 2.1, is an approximation to that used in the present work, eq. (2.9). Therefore it is worth studying what is the error made in the reconstructed phase-shifts if one uses the Lüscher equation instead of eq. (2.9). In ref. [29] it was shown that the Lüscher method can be reproduced if in eq. (2.7) one substitutes

$$I(p,s) = \frac{1}{\omega(\vec{p})} \frac{1}{s - 4\omega(\vec{p})^2}. \tag{3.1}$$

by

$$I(p,s) = \frac{1}{2\sqrt{s}} \frac{1}{p_{\rm ON}^2 - \vec{p}^{\,2}}. \tag{3.2}$$

where $p_{\rm ON} = \frac{E}{2}\sqrt{1 - \frac{4m^2}{s}}$.

In figure 8 we show the effect in the $I = 0$ phase-shifts of using the pure Lüscher method, eq. (3.2), instead of eq. (3.1). (For the isospin 2 case the effect is small and thus we do not show any plot.) The difference is significant only for phase-shifts extracted from level 2 of figure 3 since the difference is only relevant for small values of L. Therefore we only plot results extracted from level 2. The difference between our method and the Lüscher one is similar for all the three different models for the potential. The size of the difference is similar to the one from the L dependence of the potential discussed above but goes in the opposite direction. Therefore they tend to compensate each other by chance.

JHEP08(2012)071

4 Summary

In this paper we have faced the problem of the presence of the left-hand cut of the $\pi\pi$ amplitude for the evaluation of phase-shifts from lattice QCD results using Lüscher's approach. The nonperturbative approach, the study for energies different than threshold and the study of the $I = 0$ $\pi\pi$ system are done in the present work for the first time in the literature. The $t-$ and $u-$channel terms can be taken into account in a field theoretical approach by means of the IAM, or NLO N/D methods, leading to good reproductions of the scattering data. Results from lattice QCD should contain all the dynamics and, as a consequence, should account for these effects too. However, the method to go from the discrete energy level in a box from lattice simulations to the phase shifts for scattering in the infinite volume case requires the use of Lüscher's approach, or its improved version of [29], both of which rely upon the existence of a volume independent potential. Yet, the terms contributing to the left-hand cut, containing loops in the $t-$ and $u-$channels, are explicitly volume dependent. In this work we have investigated the errors induced by making use of [30] or [29] in the reproduction of phase-shifts from the energy spectrum of lattice calculations in the finite box by evaluating the volume dependence of the $\pi\pi$ scattering amplitude in one-loop ChPT. The latter is then implemented in non-perturbative methods to extract the final partial wave amplitudes. We have found that in the case of $\pi\pi$ scattering in s-wave, both for $I = 0$ and $I = 2$, the effect of the L dependence in the potential is smaller than the typical errors from the experimental phase-shifts or the differences between the three models that we have used, the IAM, NLO N/D and LO BS. This is good news for lattice calculations since one of the warnings not to go to small values of L was the possible L dependence of the potential which in some cases, like in the present one, we know that it exists. We found that it is quite safe to ignore this dependence for $L > 2.5m_\pi^{-1}$, and even with values of L around $1.5 - 2m_\pi^{-1}$ the errors induced are of the order of 5%.

On the other hand we have quantified the error made by using the pure Lüscher formula instead of the more accurate one of eq. (2.9). The effect in the phase-shifts of this approximation tends to compensate, by chance, the effect of neglecting the L dependence in the potential discussed so far.

All these findings, together with the use of the approach of [29] that also eliminates L depended terms (exponentially suppressed) from the Lüscher's approach, can encourage the performance of lattice calculations with smaller size boxes with the consequent economy in the computing time.

Acknowledgments

This work is partly supported by DGICYT contracts FIS2006-03438, the Generalitat Valenciana in the program Prometeo 2009/09, MEC FPA2010-17806, the Fundación Séneca 11871/PI/090 and the EU Integrated Infrastructure Initiative Hadron Physics Project under Grant Agreement n.227431.

JHEP08(2012)071

References

[1] Y. Nakahara, M. Asakawa and T. Hatsuda, *Hadronic spectral functions in lattice QCD*, *Phys. Rev.* **D 60** (1999) 091503 [hep-lat/9905034] [INSPIRE].

[2] K. Sasaki, S. Sasaki and T. Hatsuda, *Spectral analysis of excited nucleons in lattice QCD with maximum entropy method*, *Phys. Lett.* **B 623** (2005) 208 [hep-lat/0504020] [INSPIRE].

[3] N. Mathur et al., *Scalar Mesons $a_0(1450)$ and $\sigma(600)$ from Lattice QCD*, *Phys. Rev.* **D 76** (2007) 114505 [hep-ph/0607110] [INSPIRE].

[4] S. Basak et al., *Lattice QCD determination of patterns of excited baryon states*, *Phys. Rev.* **D 76** (2007) 074504 [arXiv:0709.0008] [INSPIRE].

[5] J. Bulava et al., *Nucleon, Δ and Ω excited states in $N_f = 2 + 1$ lattice QCD*, *Phys. Rev.* **D 82** (2010) 014507 [arXiv:1004.5072] [INSPIRE].

[6] C. Morningstar et al., *The excited hadron spectrum in lattice QCD using a new method of estimating quark propagation*, *AIP Conf. Proc.* **1257** (2010) 779 [arXiv:1002.0818] [INSPIRE].

[7] J. Foley et al., *Multi-hadron states in Lattice QCD spectroscopy*, *AIP Conf. Proc.* **1257** (2010) 789 [arXiv:1003.2154] [INSPIRE].

[8] M.G. Alford and R. Jaffe, *Insight into the scalar mesons from a lattice calculation*, *Nucl. Phys.* **B 578** (2000) 367 [hep-lat/0001023] [INSPIRE].

[9] SCALAR collaboration, T. Kunihiro et al., *Scalar mesons in lattice QCD*, *Phys. Rev.* **D 70** (2004) 034504 [hep-ph/0310312] [INSPIRE].

[10] F. Okiharu et al., *Tetraquark and pentaquark systems in lattice QCD*, hep-ph/0507187 [INSPIRE].

[11] H. Suganuma, K. Tsumura, N. Ishii and F. Okiharu, *Lattice QCD evidence for exotic tetraquark resonance*, PoS(LAT2005)070 [hep-lat/0509121] [INSPIRE].

[12] H. Suganuma, K. Tsumura, N. Ishii and F. Okiharu, *Tetra-quark resonances in lattice QCD*, *Prog. Theor. Phys. Suppl.* **168** (2007) 168 [arXiv:0707.3309] [INSPIRE].

[13] UKQCD collaboration, C. McNeile and C. Michael, *Properties of light scalar mesons from lattice QCD*, *Phys. Rev.* **D 74** (2006) 014508 [hep-lat/0604009] [INSPIRE].

[14] UKQCD collaboration, A. Hart, C. McNeile, C. Michael and J. Pickavance, *A lattice study of the masses of singlet 0++ mesons*, *Phys. Rev.* **D 74** (2006) 114504 [hep-lat/0608026] [INSPIRE].

[15] H. Wada et al., *Lattice study of low-lying nonet scalar mesons in quenched approximation*, *Phys. Lett.* **B 652** (2007) 250 [hep-lat/0702023] [INSPIRE].

[16] S. Prelovsek, C. Dawson, T. Izubuchi, K. Orginos and A. Soni, *Scalar meson in dynamical and partially quenched two-flavor QCD: Lattice results and chiral loops*, *Phys. Rev.* **D 70** (2004) 094503 [hep-lat/0407037] [INSPIRE].

[17] S. Prelovsek et al., *Searching for tetraquarks on the lattice*, *Conf. Proc.* **C 0908171** (2009) 508 [arXiv:1002.0193] [INSPIRE].

[18] S. Prelovsek et al., *Lattice study of light scalar tetraquarks with $I = 0, 2, 1/2, 3/2$: are σ and κ tetraquarks?*, *Phys. Rev.* **D 82** (2010) 094507 [arXiv:1005.0948] [INSPIRE].

JHEP08(2012)071

[19] Hadron Spectrum collaboration, H.-W. Lin et al., *First results from $2+1$ dynamical quark flavors on an anisotropic lattice: light-hadron spectroscopy and setting the strange-quark mass*, *Phys. Rev.* **D 79** (2009) 034502 [arXiv:0810.3588] [INSPIRE].

[20] C. Gattringer et al., *Hadron spectroscopy with dynamical chirally improved fermions*, *Phys. Rev.* **D 79** (2009) 054501 [arXiv:0812.1681] [INSPIRE].

[21] BGR collaboration, G.P. Engel, C. Lang, M. Limmer, D. Mohler and A. Schafer, *Meson and baryon spectrum for QCD with two light dynamical quarks*, *Phys. Rev.* **D 82** (2010) 034505 [arXiv:1005.1748] [INSPIRE].

[22] M. Mahbub, W. Kamleh, D.B. Leinweber, A. O Cais and A.G. Williams, *Ordering of spin-$\frac{1}{2}$ excitations of the nucleon in lattice QCD*, *Phys. Lett.* **B 693** (2010) 351 [arXiv:1007.4871] [INSPIRE].

[23] R.G. Edwards, J.J. Dudek, D.G. Richards and S.J. Wallace, *Excited state baryon spectroscopy from lattice QCD*, *Phys. Rev.* **D 84** (2011) 074508 [arXiv:1104.5152] [INSPIRE].

[24] C. Lang, D. Mohler, S. Prelovsek and M. Vidmar, *Coupled channel analysis of the ρ meson decay in lattice QCD*, *Phys. Rev.* **D 84** (2011) 054503 [arXiv:1105.5636] [INSPIRE].

[25] S. Prelovsek, C.B. Lang, D. Mohler and M. Vidmar, *Decay of ρ and $a1$ mesons on the lattice using distillation*, PoS(LATTICE 2011)137

[26] Z. Fodor and C. Hölbling, *Light hadron masses from lattice QCD*, *Rev. Mod. Phys.* **84** (2012) 449 [arXiv:1203.4789] [INSPIRE].

[27] V. Bernard, U.-G. Meissner and A. Rusetsky, *The Δ-resonance in a finite volume*, *Nucl. Phys.* **B 788** (2008) 1 [hep-lat/0702012] [INSPIRE].

[28] V. Bernard, M. Lage, U.-G. Meissner and A. Rusetsky, *Resonance properties from the finite-volume energy spectrum*, *JHEP* **08** (2008) 024 [arXiv:0806.4495] [INSPIRE].

[29] M. Döring, U.-G. Meissner, E. Oset and A. Rusetsky, *Unitarized chiral perturbation theory in a finite volume: scalar meson sector*, *Eur. Phys. J.* **A 47** (2011) 139 [arXiv:1107.3988] [INSPIRE].

[30] M. Lüscher, *Volume dependence of the energy spectrum in massive quantum field theories. 2. Scattering states*, *Commun. Math. Phys.* **105** (1986) 153 [INSPIRE].

[31] M. Lüscher, *Two particle states on a torus and their relation to the scattering matrix*, *Nucl. Phys.* **B 354** (1991) 531 [INSPIRE].

[32] C. Liu, X. Feng and S. He, *Two particle states in a box and the S-matrix in multi-channel scattering*, *Int. J. Mod. Phys.* **A 21** (2006) 847 [hep-lat/0508022] [INSPIRE].

[33] M. Lage, U.-G. Meissner and A. Rusetsky, *A method to measure the antikaon-nucleon scattering length in lattice QCD*, *Phys. Lett.* **B 681** (2009) 439 [arXiv:0905.0069] [INSPIRE].

[34] V. Bernard, M. Lage, U.-G. Meissner and A. Rusetsky, *Scalar mesons in a finite volume*, *JHEP* **01** (2011) 019 [arXiv:1010.6018] [INSPIRE].

[35] M. Döring, J. Haidenbauer, U.-G. Meissner and A. Rusetsky, *Dynamical coupled-channel approaches on a momentum lattice*, *Eur. Phys. J.* **A 47** (2011) 163 [arXiv:1108.0676] [INSPIRE].

[36] A. Martinez Torres, L. Dai, C. Koren, D. Jido and E. Oset, *The KD, ηD_s interaction in finite volume and the nature of the $D^*_{s0}(2317)$ resonance*, *Phys. Rev.* **D 85** (2012) 014027 [arXiv:1109.0396] [INSPIRE].

JHEP08(2012)071

[37] M. Döring and U.G. Meissner, *Finite volume effects in pion-kaon scattering and reconstruction of the $\kappa(800)$ resonance*, *JHEP* **01** (2012) 009 [arXiv:1111.0616] [INSPIRE].

[38] L. Roca and E. Oset, *Scattering of unstable particles in a finite volume: the case of $\pi\rho$ scattering and the $a_1(1260)$ resonance*, *Phys. Rev.* **D 85** (2012) 054507 [arXiv:1201.0438] [INSPIRE].

[39] J.-J. Xie and E. Oset, *The DN, $\pi\Sigma_c$ interaction in finite volume and the $\Lambda_c(2595)$ resonance*, arXiv:1201.0149 [INSPIRE].

[40] H.-X. Chen and E. Oset, *The pion-pion interaction in the ρ channel in finite volume*, arXiv:1202.2787 [INSPIRE].

[41] A. Martinez Torres, M. Bayar, D. Jido and E. Oset, *Strategy to find the two $\Lambda(1405)$ states from lattice QCD simulations*, arXiv:1202.4297 [INSPIRE].

[42] J. Oller, E. Oset and A. Ramos, *Chiral unitary approach to meson meson and meson-baryon interactions and nuclear applications*, *Prog. Part. Nucl. Phys.* **45** (2000) 157 [hep-ph/0002193] [INSPIRE].

[43] J. Oller and E. Oset, *N/D description of two meson amplitudes and chiral symmetry*, *Phys. Rev.* **D 60** (1999) 074023 [hep-ph/9809337] [INSPIRE].

[44] J. Oller and U.G. Meissner, *Chiral dynamics in the presence of bound states: kaon nucleon interactions revisited*, *Phys. Lett.* **B 500** (2001) 263 [hep-ph/0011146] [INSPIRE].

[45] Z.-H. Guo and J. Oller, *Resonances from meson-meson scattering in* U(3) *CHPT*, *Phys. Rev.* **D 84** (2011) 034005 [arXiv:1104.2849] [INSPIRE].

[46] T.N. Truong, *Chiral perturbation theory and final state theorem*, *Phys. Rev. Lett.* **61** (1988) 2526 [INSPIRE].

[47] T.N. Truong, *Remarks on the unitarization methods*, *Phys. Rev. Lett.* **67** (1991) 2260 [INSPIRE].

[48] A. Dobado, M.J. Herrero and T.N. Truong, *Unitarized chiral perturbation theory for elastic pion-pion scattering*, *Phys. Lett.* **B 235** (1990) 134 [INSPIRE].

[49] A. Dobado and J. Pelaez, *A global fit of $\pi\pi$ and πK elastic scattering in ChPT with dispersion relations*, *Phys. Rev.* **D 47** (1993) 4883 [hep-ph/9301276] [INSPIRE].

[50] A. Dobado and J. Pelaez, *The inverse amplitude method in chiral perturbation theory*, *Phys. Rev.* **D 56** (1997) 3057 [hep-ph/9604416] [INSPIRE].

[51] J. Oller, E. Oset and J. Pelaez, *Meson meson interaction in a nonperturbative chiral approach*, *Phys. Rev.* **D 59** (1999) 074001 [*Erratum ibid.* **D 60** (1999) 099906] [hep-ph/9804209] [INSPIRE].

[52] S.R. Beane et al., *Precise determination of the $I = 2\pi\pi$ scattering length from mixed-action lattice QCD*, *Phys. Rev.* **D 77** (2008) 014505 [arXiv:0706.3026] [INSPIRE].

[53] NPLQCD collaboration, S. Beane et al., *The $I = 2\pi\pi$ S-wave scattering phase shift from lattice QCD*, *Phys. Rev.* **D 85** (2012) 034505 [arXiv:1107.5023] [INSPIRE].

[54] J.J. Dudek, R.G. Edwards and C.E. Thomas, *S and D-wave phase shifts in isospin-2 $\pi\pi$ scattering from lattice QCD*, arXiv:1203.6041 [INSPIRE].

[55] P.F. Bedaque, I. Sato and A. Walker-Loud, *Finite volume corrections to pi-pi scattering*, *Phys. Rev.* **D 73** (2006) 074501 [hep-lat/0601033] [INSPIRE].

JHEP08(2012)071

[56] Particle Data Group collaboration, J. Beringer et al., *Review of Particle Physics*, *Phys. Rev.* **D 86** (2012) 010001.

[57] M. Albaladejo and J. Oller, *Identification of a scalar glueball*, *Phys. Rev. Lett.* **101** (2008) 252002 [arXiv:0801.4929] [INSPIRE].

[58] M. Albaladejo, J. Oller and L. Roca, *Dynamical generation of pseudoscalar resonances*, *Phys. Rev.* **D 82** (2010) 094019 [arXiv:1011.1434] [INSPIRE].

[59] M. Albaladejo and J.A. Oller, *Nucleon-nucleon interactions from dispersion relations: Elastic partial waves*, *Phys. Rev.* **C 84** (2011) 054009 [arXiv:1107.3035] [INSPIRE].

[60] M. Albaladejo and J.A. Oller, *Nucleon-nucleon interactions from dispersion relations: coupled partial waves*, arXiv:1201.0443 [INSPIRE].

[61] J. Oller and E. Oset, *Chiral symmetry amplitudes in the S wave isoscalar and isovector channels and the sigma, f0(980), a0(980) scalar mesons*, *Nucl. Phys.* **A 620** (1997) 438 [*Erratum ibid.* **A 652** (1999) 407] [hep-ph/9702314] [INSPIRE].

[62] J. Gasser and H. Leutwyler, *Chiral perturbation theory to one loop*, *Annals Phys.* **158** (1984) 142 [INSPIRE].

[63] E. Oset, A. Ramos and C. Bennhold, *Low lying $S = -1$ excited baryons and chiral symmetry*, *Phys. Lett.* **B 527** (2002) 99 [*Erratum ibid.* **B 530** (2002) 260] [nucl-th/0109006] [INSPIRE].

[64] A. Gomez Nicola, J. Pelaez and G. Rios, *The inverse amplitude method and Adler zeros*, *Phys. Rev.* **D 77** (2008) 056006 [arXiv:0712.2763] [INSPIRE].

[65] C. Hanhart, J. Pelaez and G. Rios, *Quark mass dependence of the ρ and σ from dispersion relations and chiral perturbation theory*, *Phys. Rev. Lett.* **100** (2008) 152001 [arXiv:0801.2871] [INSPIRE].

[66] M. Albaladejo and J. Oller, *Size of the σ meson and its nature*, *Phys. Rev.* **D 86** (2012) 034003 [arXiv:1205.6606] [INSPIRE].

[67] G.F. Chew and S. Mandelstam, *Theory of low-energy pion pion interactions*, *Phys. Rev.* **119** (1960) 467 [INSPIRE].

[68] A. Lacour, J. Oller and U.-G. Meissner, *Non-perturbative methods for a chiral effective field theory of finite density nuclear systems*, *Annals Phys.* **326** (2011) 241 [arXiv:0906.2349] [INSPIRE].

[69] D. Jido, J. Oller, E. Oset, A. Ramos and U. Meissner, *Chiral dynamics of the two $\Lambda(1405)$ states*, *Nucl. Phys.* **A 725** (2003) 181 [nucl-th/0303062] [INSPIRE].

[70] B. Hyams et al., *$\pi\pi$ phase shift analysis from 600 MeV to 1900 MeV*, *Nucl. Phys.* **B 64** (1973) 134 [INSPIRE].

[71] R. Kaminski, L. Lesniak and K. Rybicki, *Separation of S wave pseudoscalar and pseudovector amplitudes in $\pi^- p$ (polarized) $\to \pi^+\pi^- n$ reaction on polarized target*, *Z. Phys.* **C 74** (1997) 79 [hep-ph/9606362] [INSPIRE].

[72] G. Grayer et al., *High statistics study of the reaction $\pi^- p \to \pi^-\pi^+ n$: apparatus, method of analysis and general features of results at 17 GeV/c*, *Nucl. Phys.* **B 75** (1974) 189 [INSPIRE].

[73] BNL-E865 collaboration, S. Pislak et al., *A new measurement of $K^+(e4)$ decay and the S wave $\pi\pi$ scattering length $a_0(0)$*, *Phys. Rev. Lett.* **87** (2001) 221801 [*Erratum ibid.* **105** (2010) 019901] [hep-ex/0106071] [INSPIRE].

JHEP08(2012)071

[74] S. Pislak et al., *High statistics measurement of $K(e4)$ decay properties*, *Phys. Rev.* **D 67** (2003) 072004 [*Erratum ibid.* **D 81** (2010) 119903] [hep-ex/0301040] [INSPIRE].

[75] L. Masetti, *Measurements of $K(e4)$ and $K^{\pm} \to \pi^0\pi^0\pi^{\pm}$ decays*, hep-ex/0610071 [INSPIRE].

[76] M. Losty et al., *A study of $\pi^-\pi^-$ scattering from π^-p interactions at 3.93 GeV/c*, *Nucl. Phys.* **B 69** (1974) 185 [INSPIRE].

[77] W. Hoogland et al., *Measurement and analysis of the $\pi^+\pi^+$ system produced at small momentum transfer in the reaction $\pi^+p \to \pi^+\pi^+n$ at 12.5 GeV*, *Nucl. Phys.* **B 126** (1977) 109 [INSPIRE].

JHEP08(2012)071